Asian Journal of Chemistry; Vol. 35, No. 6 (2023), 1533-1538

ASIAN JOURNAL OF CHEMISTRY

https://doi.org/10.14233/ajchem.2023.27843

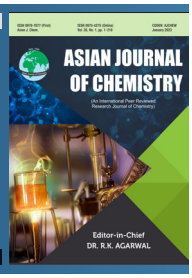

Synthesis and Characterization of SnO_2/BNNTs Nanocomposite for Ethanol Vapour Sensing at Room Temperature

H. SHARMA[1,*], P.S. RAWAT[1], B.S. RAWAT[1], N. KUMAR[1] and S. VERMA[2]

[1]Department of Physics, School of Applied & Life Sciences, Uttaranchal University, Premnagar, Dehradun-248007, India
[2]Department of Biotechnology, School of Applied & Life Sciences, Uttaranchal University, Premnagar, Dehradun-248007, India

*Corresponding author: E-mail: hemlatasharma208@gmail.com

Received: 5 April 2023; *Accepted*: 20 May 2023; *Published online*: 27 May 2023; AJC-21273

Ethanol vapour sensors based on tin oxide (SnO_2) nanoparticles onto boron nitride nanotubes (BNNTs) have been synthesized as a promising solution for detecting ethanol vapour in air. The existence of encapsulation of BNNTs over SnO_2 *i.e.* SnO_2/BNNT was confirmed by AFM, FTIR and current-voltage characteristics. Activation energy of sensor has been investigated to study the nature of synthesized material. Ethanol sensitivity, responsiveness and response-recovery durations of the SnO_2-BNNTs sensor, as well as other sensing features, was examined by exposure to various ethanol vapour concentrations starting from 70 to 500 mL/min at room temperature with increasing rate of pressure value at room temperature. The SnO_2 nanoparticles have a high sensitivity to ethanol vapour, while BNNTs enhance the sensing performance and stability of the sensor. This is achieved by combining BNNT (large surface area) and SnO_2 (good electrical conductivity). The ethanol vapour sensor based on SnO_2-BNNTs has been shown to have a good response and recovery time around 1 min and 2 s, respectively. With its high sensitivity of ~110 and stability, it is an excellent option for practical applications.

Keywords: Ethanol vapour, Sensitivity, Tin oxide, Boron nitride nanotubes, Nanocomposites.

INTRODUCTION

SnO_2-boron nitride nanotubes (BNNTs) are being used as the basis for ethanol vapour sensor, since SnO_2 is a good material for sensing ethanol vapours due to its high sensitivity and fast response time, while BNNTs improves the stability and selectivity of the sensor [1]. The sensor operates by measuring changes in electrical conductivity that occur when ethanol vapours are present, which is then translated into a corresponding change in resistance [2,3]. Ethanol sensors have been found to be highly selective, stable and accurate, which makes them promising material for variety of applications including breath analyzer, industrial process control and environmental monitoring, automotive industry, medical applications, *etc*. These can be used to determine presence of ethanol in breathalyzer devices and to check its concentration in a person's breath, which can indicate their level of drunkenness [3]. The nanocomposite of SnO_2 and BNNT are formed by mixing both of them through *in situ* or *ex situ* method for sensing applications because of their synergistic effect, they have unique and wide variety of properties that complement each other [1,2].

SnO_2, commonly used in gas sensing due to its high sensitivity, fast response and low cost. But due to shortcomings of its stability and durability, it can be used to make its composite with some other material [3,4]. Boron nitride nanotubes (BNNTs), on the other hand, are highly stable and durable materials with excellent electrical and thermal conductivity due to large surface area and volume ratio and high aspect ratio [5,6]. When SnO_2 is mixed with BNNTs, the resulting nanocomposite material can exhibit improved sensing performance compared to either material alone and can be used for many applications too. The BNNTs can enhance the stability and durability of the sensing material [7], while the SnO_2 provides high sensitivity and fast response [8]. Additionally, the high surface area of the BNNTs can provide more active sites for sensing, leading to improved sensitivity [9-11]. In short, the combination of SnO_2 and BNNT in a composite material can result in improved sensing performance, making it a promising material for various sensing applications [12]. The synthesized nanocomposite sensor have high thermal stability and electrical conductivity, making them suitable for room temperature sensing applications such as gas sensing, humidity sensing and pressure sensing.

EXPERIMENTAL

Boron nitride nanotubes (BNNTs) (15-20 nm in diameter) were used and tin chloride dihydrate ($SnCl_2 \cdot 2H_2O$) was purchased from Sigma-Aldrich, USA with purity of 99%. Acetone and ethanol were purchased from Fisher-Scientific Ltd. Remaining precursors and chemicals were used without purification and were purchased from Sigma-Aldrich. Deionised water was used in the experiment.

General procedure for synthesis of BNNT solution and SnO_2/BNNT nanocomposite: BNNTs were dispersed by mixing 0.001 g of BNNTs with 10 mL of ethanol. Then sonication of solution was done for 3 h at room temperature (18 ºC) in order to achieve complete dispersion and to lessen nanotube clumping (750 W Ultrasonic Processor + microtip at 20% amplitude, Sonics & Materials). For nanocomposite, 0.008 g from $SnCl_4 \cdot 2H_2O$ was used and mixed with 10 mL of ethanol. The resulting solution $Sn(OH)_2$ was treated by sonication method for 20 min. In order to create a homogeneous film, $Sn(OH)_2$ solution was added to BNNTs/ethanol combination before the nanocomposite mixture was quickly sonicated before drop casting. The SnO_2/BNNTs nanocomposite film was created by oxidizing the nanocomposite at 500 ºC in dry flowing oxygen after the deposition of nanocomposite onto the electrodes and dried at ambient temperature.

Characterization: For an AFM data, a Dimension Model D3100V (Veeco) atomic force microscope and NanoscopeV controller (Bruker) was used. Also an "E" scanner was used to acquire AFM data and its calculations. Atomic force microscopy (AFM) Image results and analysis was performed with NanoscopeV analysis software (version 1.5). Using a thermal chuck system on the probe station (Cascade Microtech with a B1500A parameter analyzer, Agilent) (Model ETC-200L, ESPEC), V/I measurements at various temperatures were taken. An FTIR spectrophotometer (Shimadzu) was used to record FTIR spectra. The fabrication of electronic devices for the two-terminal electrical characterization of SnO_2-boron nitride (SnO_2/BNNTs) nanocomposites and vapour sensing studies utilized platinum electrodes (Smart Microsystems Pt MB-4000, Windsor Scientific Ltd. Slough, UK). Platinum electrodes were patterned on the top of the SiO_2 layer. The 4 electrodes of width 10 µm with 10 µm spaces between them were cleaned by rinsing with ethanol and dried in a stream of nitrogen gas. The synthesized SnO_2/BNNTs nanocomposites film was deposited by micropipette over surface of electrodes. On exposure to ethanol vapour, 4 electrodes of platinum was electrically connected and electrical resistance was measured using a normal digital multimeter (DMM) and ethanol vapour sensing was carried out.

RESULTS AND DISCUSSION

Fig. 1 demonstrates 2D AFM image of the synthesized SnO_2-BNNTs. The surface morphology of the synthesized nanomaterials gives a good indication for formation of SnO_2/BNNTs with average vertical particle size of about 40 nm. Small dots of AFM image assigned to the SnO_2 nanoparticles having diameter of ~10 nm and short tubes of BNNTs/SnO_2 having diameter of ~30-40 nm. Diameter of synthesized nanocomposite sample increases that shows encapsulation of BNNTs over SnO_2. The AFM image can provide information on the size, shape and arrangement of the SnO_2 particles on the BNNT surface. Additionally, AFM can also be used to measure the mechanical and electrical properties of the SnO_2/BNNT sample.

The I-V curve of SnO_2/BNNTs at various temperatures is shown in Fig. 2. Response to a minor voltage (ranging from -2V to 2V) was studied throughout the temperature range (300-400 K). The I-V (current-voltage) characteristics of SnO_2 and BNNT based devices can vary based on the specific device configuration, materials used and operating conditions. A change in mechanical straining as the temperature is increased

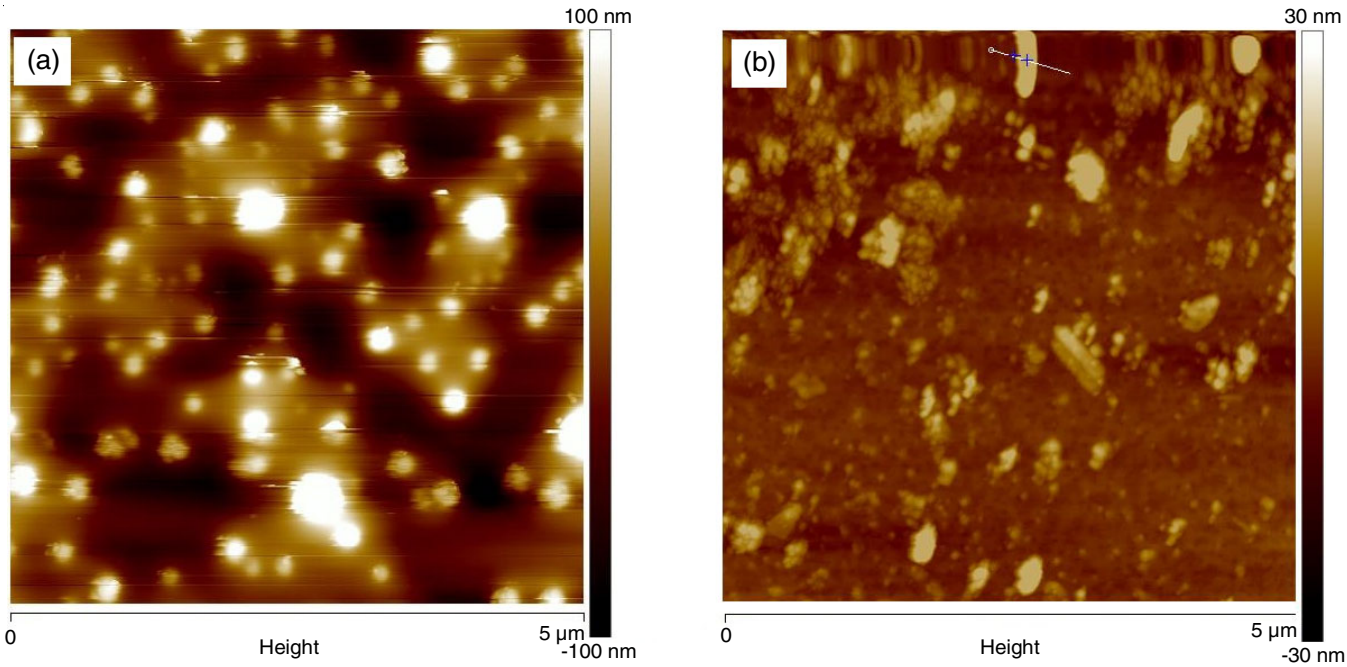

Fig. 1. AFM image of (a) SnO_2 (b) SnO_2/BNNTs nanocomposite

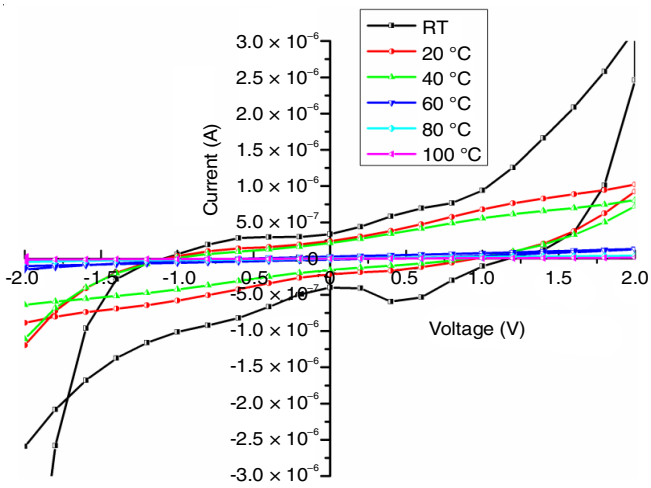

Fig. 2. I-V curves of SnO_2/BNNTs nanocomposite

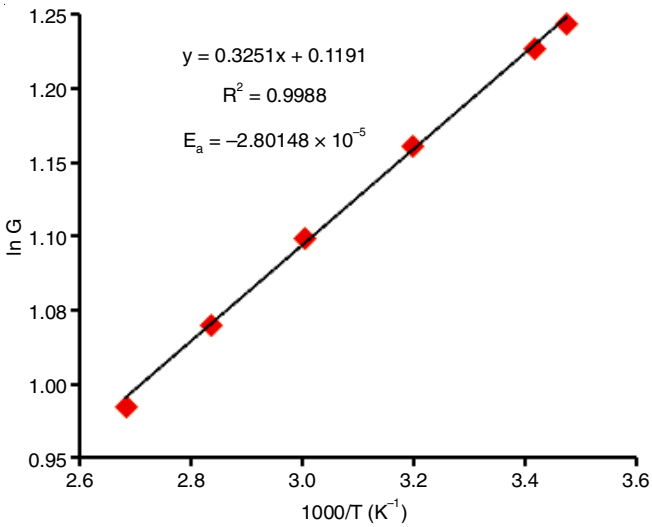

Fig. 3. Arrhenius plot of temperature-dependent resistance of SnO_2/BNNTs nanocomposite

from room temperature to 100 ºC. Due to heterojunction formation, SnO_2/BNNT nanocomposite exhibited rectifying ehaviour at the interface between different phases or materials within the nanocomposite suggesting the formation of a rectifying Schottky junction [13,14]. However, in general, SnO_2 can exhibit n-type behaviour due to its intrinsic defects or impurities and is commonly used as the sensing material in gas sensors. BNNT, on the other hand, is an electrically insulating material, but it can exhibit p-type ehaviour when doped with suitable impurities [15,16]. For a typical p-n junction device, the I-V curve can exhibit a rectifying behaviour, with a large resistance in the reverse-bias direction and a smaller resistance in the forward-bias direction.

This is due to the built-in potential created by the p-n junction, which allows for majority carrier flow in one direction and blocks it in the other direction [17]. When electric field is applied, mobility of charge carriers (*e.g.*, electrons or holes) to move through the material increases. And as the temperature increased, the mobility of carriers in the tin oxide/boron nitride nanocomposite material may increase due to enhanced thermal energy, allowing them to move more freely. This increased mobility may result in a reduced rectification ehaviour as the carriers can more easily traverse the interface between the tin oxide and boron nitride components, leading to a decrease in the rectifying behaviour of the material. Overall, the nature of the I-V curve of SnO_2/BNNT depends on various factors, but it is usually characterized by good rectifying ehaviour and a steep slope at low voltages and a gradual slope at high voltages.

Fig. 3 shows the Arrhenius plot of SnO_2/BNNT, which refers to a graphical representation of the relationship between the reaction rate of the material and temperature. The slope of the plot provides information about the activation energy of the reaction, while the intercept gives an estimate of the pre-exponential factor was used to analyze the temperature-dependence of the catalytic activity of SnO_2/BNNTs and can provide important insights into the mechanism of the reaction and ensures that the material is semiconductor. The Arrhenius plots of ln G as a function of reciprocal absolute temperature (1000/T) at reduced pressure (~ 10^{-2} torr) is showing a linear relationship, which means that the reaction is thermally activated. The nano-composite reaction has well-defined activation energy (-2.8 × 10^{-5} eV) and follows simple exponential temperature dependence. The slope of the straight line represents the negative of the activation energy divided by the gas constant (E_a/R), while the intercept on the y-axis represents the natural logarithm of the pre-exponential factor or frequency factor (ln(G)).

FTIR studies: Fig. 4 shows the FTIR spectrum of SnO_2/BNNT nanocomposite at definite frequencies that correspond to the vibrational modes of the chemical bonds present in the material. The SnO_2/BNNTs nanocomposite typically exhibits peaks in the region of 3000-600 cm^{-1}, which are associated with the stretching vibrations of Sn-O and B-N bonds [18]. The FTIR spectrum of SnO_2/BNNTs nanocomposite is also affected by various factors, such as the synthesis method, doping level, temperature and humidity. These factors can cause changes in the intensity, position and shape of the peaks, which can provide additional information about the material's properties. The FTIR peak at 1100 cm^{-1} could corresponds to the stretching vibration of Sn-O bonds, indicating the presence of SnO_2 in the nanocomposite. The FTIR peak at 1100 cm^{-1} could also indicate the formation of a chemical bond or interaction between

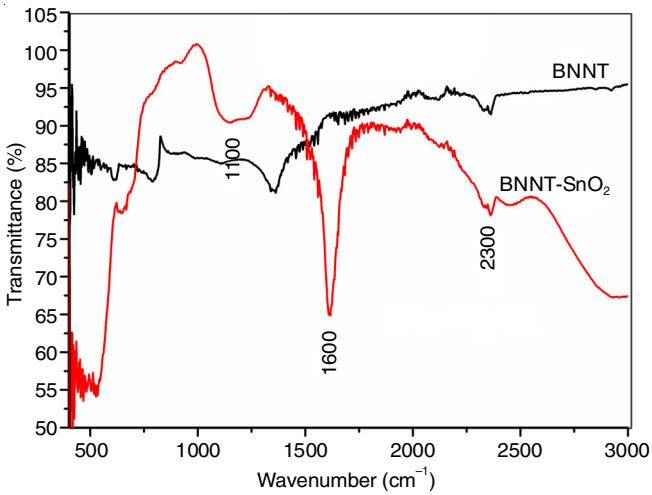

Fig. 4. FTIR spectra of BNNT and BNNT-SnO_2

SnO_2 and BNNTs, suggesting the successful formation of the SnO_2/BNNT nanocomposite [19]. The peaks in the FTIR spectra of SnO_2/BNNT at 1600-1500 cm^{-1} are typically assigned to the bending vibrations of the Sn-O bonds in the SnO_2 nanostructures [17]. The presence of BN nanotubes may influence the intensity and position of these peaks. The peaks of SnO_2/BNNT at 2500-2000 cm^{-1} are typically assigned to the stretching vibrations of the B-N bonds in the BN nanotubes.

Chronoamperometry studies: The chronoamperometry detection (CA) of SnO_2/MWCNTs nanocomposite material at room temperature is shown in Fig. 5. To create electronic devices for two-terminal electrical characterization of SnO_2-boron nitride (SnO_2/BNNTs) nanocomposites for vapour sensing investigations, platinum electrodes were used. The top of the SiO_2 layer was imprinted using platinum electrodes. The four electrodes, each 10 mm wide and separated by 10 mm, were cleaned by ethanol rinsing and dried in a stream of nitrogen gas. The synthesized SnO_2/BNNTs nanocomposites film was deposited by micropipette over surface of electrodes. Electrical contact was created between nearby electrodes during sensing studies. When the exposure concentration of ethanol is low, we observed a gradual increase in the electrical current with time. This indicates an increase in electrical conductivity of the SnO_2/BNNT composite material as ethanol acts as a dopant, introducing charge carriers and enhancing the conductivity. At higher concentration of ethanol, it is observed the largest electrical current or the largest electrical conductivity of the SnO_2/BNNT composite material *i.e.* they exhibited a higher sensitivity to ethanol at higher concentrations, with response times of the order of several seconds. The current generated by the SnO_2/BNNTs in response to a change in ethanol concentration can be several orders of magnitude higher than that of other metal oxide sensors. Additionally, the use of BNNTs as a support for SnO_2 can improve the sensing performance of the SnO_2 by increasing its surface area and reducing the electron-hole recombination rate. The sensitivity of SnO_2/BNNTs for ethanol vapour sensing refers to the ability of the sensors to accurately detect changes in the concentration of ethanol vapour in the surrounding environment. The sensitivity of SnO_2/BNNTs for ethanol sensing is influenced by several factors, including the composition and structure of the SnO_2/BNNTs, the operating temperature, the concentration of ethanol and the applied voltage. In general, SnO_2/BNNTs have been found to have a high sensitivity to ethanol, with a very low detection. At further high concentration of ethanol vapour at room temperature we can calculate and find out the optimal concentration for enhancing its electrical conductivity [20].

Comparative studies: Table-1 shows the comparison of sensing characteristics of various metal oxides and nanocomposites for ethanol vapour. Exposure of ethanol vapours for sensing properties of PANI/SnO_2 at 30, 60 and 90 ºC had been reported by Geng *et al.* [23]. It has been found that at elevated temperatures *i.e.* at 90 ºC, the sensitivity towards vapours (100 ppm) was observed with response/recovery times of 43s/48 s. However in this work for synthesized nanocomposites, we obtained high sensitivity value ~110, fast response time and recovery time ~1 min and ~2 s, respectively at room temperature *i.e.*18 ºC. In PANI/TiO_2 [22], the room temperature is optimum operating temperature for highest sensitivity at 100 ppm exposure of ethanol vapours but its recovery time is quite high.

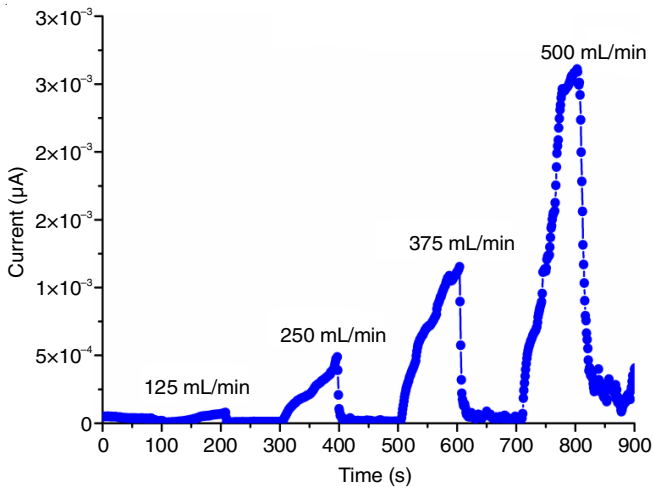

Fig. 5. Amperometric detection of SnO_2/BNNTs composite

Sensitivity: Sensitivity *vs.* pressure of SnO_2/BNNTs nanocomposite at room temperature is shown in Fig. 6. The graph reveals that the sensitivity increases gradually at first as vapour concentration rises but later on at high concentrations of ethanol vapour (pressure ~6.05 Pa), it increases rapidly. The sensitivity of SnO_2/BNNTs composites to ethanol can be improved by the addition of BNNTs, which can increase the surface area of the composite and reduce the electron-hole recombination rate. The sensitivity of SnO_2/BNNTs composites to the pressure change can be influenced by the degree of dispersion of BNNTs in the SnO_2 matrix. Thus improving dispersion of the BNNTs can lead to a higher sensitivity. The pressure response of SnO_2/BNNTs composites for ethanol sensing can also be influenced by the operating temperature. In general, SnO_2/BNNTs composites exhibit a higher sensitivity to ethanol at higher operating temperatures. The response time of SnO_2/BNNTs composites to pressure change can range from a few milliseconds to several seconds, depending on the operating conditions and the concentration of ethanol vapour.

TABLE-1
COMPARISON OF SENSING CHARACTERISTICS OF METAL OXIDES AND NANOCOMPOSITES FOR ETHANOL VAPOUR

Sensing material	Optimum operating temperature (°C)	Sensitivity/response	Response time (s)	Recovery time (s)	Ref.
SnO_2 sensors	250	~40 at 100 ppm	15-26	42-67	[21]
SnO_2-Au sensors	175	~78 at 100 ppm	19-27	41-56	[21]
SnO_2-Pd sensors	175	~94 at 100 ppm	29-45	33-40	[21]
TiO_2	200	~20-50 at 5 ppm to 20 ppm resp.	300-200	350-385	[22]
PANI/TiO_2	Room temperature	~15-38 at 5 ppm to 20 ppm resp.	285-115	235-340	[22]

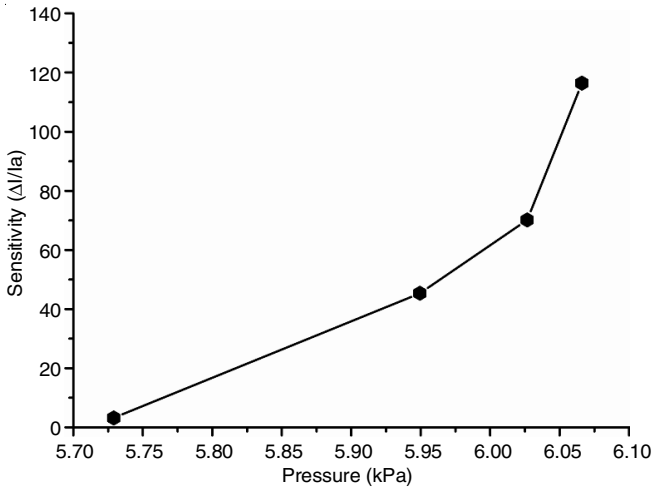

Fig. 6. Sensitivity *vs.* pressure of SnO_2/BNNTs composite

Response and recovery studies: It can be seen that the sensor SnO_2/BNNTs has a fast response time and recovery time ~1 min and ~ 2 s, respectively at sensitivity ~110 as shown in Fig. 7. At high concentrations of vapour, sensitivity and response increases rapidly and response and recovery time becomes less. SnO_2 has a high sensitivity to ethanol and its electrical conductivity increases upon exposure to the vapour [24]. This increase in conductivity can be used to detect the presence of ethanol. The sensing mechanism of SnO_2 is based on the adsorption of ethanol molecules onto the surface of the SnO_2 material, which changes the electronic properties of the material and leads to changes in its electrical conductivity [11]. This change in electrical conductivity leads to the resistance change due to the transfer of electrons from SnO_2 to the ethanol molecules and increases the mobility of charge carriers which is creating a conductive pathway for free electrons to flow through the synthesized SnO_2/BNNTs nanocomposite. This allows the detection of the presence of ethanol vapour in the atmosphere. Upon removal of the ethanol vapour, the adsorbed ethanol molecules are desorbed from the surface of the nanocomposite and the resistance of the material returns to its original state [25]. This facilitates the BNNT/SnO_2 nanocomposite for repeatable and accurate sensing of ethanol vapour.

Conclusion

Using a wet chemical method and the solution route, SnO_2/BNNTs were successfully developed. An effective encapsulation of BNNT on SnO_2 nanoparticles with an average diameter in the nanoscale regime of roughly 40-50 nm was shown by AFM image. The electrical properties of the hybrid SnO_2/BNNTs structure can be seen in the V/I values. The I-V curve of SnO_2/BNNT depends on the formation of p-n junction between them and showed a good rectifying ehaviour with a steep slope at low voltages and a gradual slope at high voltages. The Arrhenius plot of synthesized nanocomposite SnO_2/BNNTs showed a linear relationship which indicated that the reaction is thermally activated. The present study reveals that the existence of a heterojunction between a hybrid material made of tin oxide and boron nitride nanotubes can be used to explain the ethanol vapour sensing mechanism. With a high sensitivity (~ 110) at room temperature, the sensor based on synthetic nanocomposite material SnO_2/BNNTs has a good response time of approximately 1 min. The response time and recovery time of SnO_2/BNNT nanocomposite was found to be ~1 min and ~2 s, respectively when sensitivity raised by a factor of 110. At high concentrations of vapour, sensitivity and response increases rapidly and recovery time becomes less.

ACKNOWLEDGEMENTS

One of the authors, H. Sharma acknowledges to Department of Science & Technology (DST), New Delhi (India) for the financial assistance under INSPIRE Fellowship (No. DST/INSPIRE Fellowship/2013/92, Registration No: IF130149) and British council U.K. for Newton Bhabha Ph.D. placement award under Newton Bhabha Fellowship for their contributions in providing facility needed for the completion of this research work.

CONFLICT OF INTEREST

The authors declare that there is no conflict of interests regarding the publication of this article.

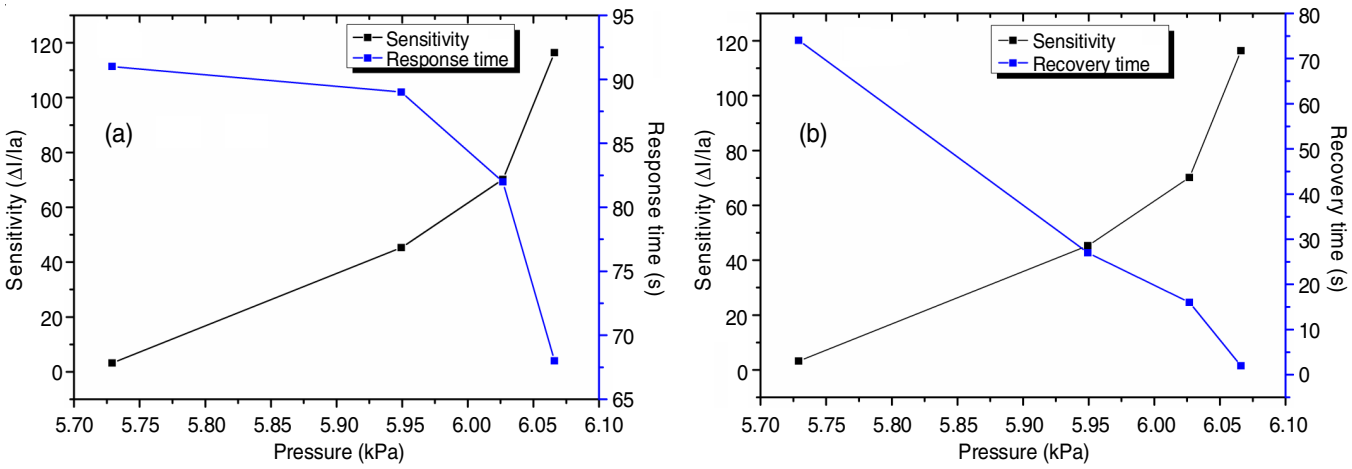

Fig. 7. Relation between sensitivity, pressure (a) response time and (b) recovery time

REFERENCES

1. B. Sharma, A. Sharma and J. Myung, *Sens. Actuators B Chem.*, **331**, 129464 (2021); https://doi.org/10.1016/j.snb.2021.129464
2. M. Yoosefian, N. Etminan, M.Z. Moghani, S. Mirzaei and S. Abbasi, *Superlatt. Microstruct.*, **98**, 325 (2016); https://doi.org/10.1016/j.spmi.2016.08.049
3. R.C. Singh, N. Kohli, M.P. Singh and O. Singh, *Bull. Mater. Sci.*, **33**, 575 (2010); https://doi.org/10.1007/s12034-010-0088-7
4. W. Tian, Y. Wang, Y. Zhang, J. Cao and R.F. Guan, *ACS Appl. Nano Mater.*, **4**, 6316 (2021); https://doi.org/10.1021/acsanm.1c01165
5. N.A. Pandit and T. Ahmad, *Molecules*, **27**, 7038 (2022); https://doi.org/10.3390/molecules27207038
6. S. Tyagi, M. Chaudhary, A.K. Ambedkar, K. Sharma, Y.K. Gautam and B.P. Singh, *Sens. Diagn.*, **1**, 106 (2022); https://doi.org/10.1039/D1SD00034A
7. K.B. Dhungana and R. Pati, *Sensors*, **14**, 17655 (2014); https://doi.org/10.3390/s140917655
8. T. Tharsika, M. Thanihaichelvan, A.S.M.A. Haseeb and S.A. Akbar, *Front. Mater.*, **6**, 122 (2019); https://doi.org/10.3389/fmats.2019.00122
9. D. Golberg, Y. Bando, Y. Huang, T. Terao, M. Mitome, C. Tang and C. Zhi, *ACS Nano*, **4**, 2979 (2010); https://doi.org/10.1021/nn1006495
10. D. Köken, M.Sc. Thesis, Synthesis and Optimization of Boron Nitride Nanotubes for Stable Aqueous Dispersions, Sabanci University, Istanbul, Turkey (2016).
11. C.H. Lee, S. Bhandari, B. Tiwari, N. Yapici, D. Zhang and Y.K. Yap, *Molecules*, **21**, 922 (2016); https://doi.org/10.3390/molecules21070922
12. W. Meng, Y. Huang, Y. Fu, Z. Wang and C. Zhi, *J. Mater. Chem. C Mater. Opt. Electron. Devices*, **2**, 10049 (2014); https://doi.org/10.1039/C4TC01998A
13. D. Zhang, N. Yapici, R. Oakley and Y.K. Yap, *J. Mater. Res.*, **37**, 4605 (2022); https://doi.org/10.1557/s43578-022-00737-5
14. H. Du, X. Li, P. Yao, J. Wang, Y. Sun and L. Dong, *Nanomaterials*, **8**, 509 (2018); https://doi.org/10.3390/nano8070509
15. S.B. Kondawar, A.M. More, H.J. Sharma and S.P. Dongre, *J. Mater. Nanosci.*, **4**, 13 (2017).
16. H.J. Sharma, D.V. Jamkar and S.B. Kondawar, *Procedia Mater. Sci.*, **10**, 186 (2015); https://doi.org/10.1016/j.mspro.2015.06.040
17. H.J. Sharma, M.A. Salorkar and S.B. Kondawar, *Adv. Mater. Process.*, **2**, 61 (2017); https://doi.org/10.5185/amp.2017/114
18. R. Haubner, M. Wilhelm, R. Weissenbacher and B. Lux, Boron Nitrides-Properties, Synthesis and Applications, Springer: Berlin Heidelberg, pp. 1-45 (2002).
19. M.J. Rand and J.F. Roberts, *J. Electrochem. Soc.*, **115**, 423 (1968); https://doi.org/10.1149/1.2411238
20. S.S. Niavol and H.M. Moghaddam, *J. Mater. Sci. Mater. Electron.*, **32**, 6550 (2021); https://doi.org/10.1007/s10854-021-05372-0
21. Y.V. Kaneti, J. Yue, J. Moriceau, C. Chen, M. Liu, Y. Yuan, X. Jiang and A. Yu, *Sens. Actuators B Chem.*, **219**, 83 (2015); https://doi.org/10.1016/j.snb.2015.04.136
22. I. Gawri, R. Ridhi, K.P. Singh and S.K. Tripathi, *Mater. Res. Express*, **5**, 025303 (2018); https://doi.org/10.1088/2053-1591/aaa9f1
23. L. Geng, Y. Zhao, X. Huang, S. Wang, S. Zhang and S. Wu, *Sens. Actuators B Chem.*, **120**, 568 (2007); https://doi.org/10.1016/j.snb.2006.03.009
24. M. Riordan and L. Hoddeson, *Res. Sec. Sci. Teach.*, **34**, 73 (2003); https://doi.org/10.1109/6.591664
25. N.C. Joshi, *Sep. Sci. Technol.*, **57**, 2420 (2022); https://doi.org/10.1080/01496395.2022.2069042